RAA 2018 Vol. **18** No. **5**, 52(12pp) doi: 10.1088/1674–4527/18/5/52

http://www.raa-journal.org *http://iopscience.iop.org/raa*

***R**esearch in*
***A**stronomy and*
***A**strophysics*

Binary Star Fractions from the LAMOST DR4

Zhi-Jia Tian[1,⋆], Xiao-Wei Liu[1,4], Hai-Bo Yuan[2], Bing-Qiu Chen[4,⋆], Mao-Sheng Xiang[2,⋆], Yang Huang[1,4,⋆], Chun Wang[1], Hua-Wei Zhang[1], Jin-Cheng Guo[1,⋆], Juan-Juan Ren[3], Zhi-Ying Huo[3], Yong Yang[4], Meng Zhang[1], Shao-Lan Bi[2], Wu-Ming Yang[2], Kang Liu[2], Xian-Fei Zhang[2], Tan-Da Li[3], Ya-Qian Wu[2] and Jing-Hua Zhang[2]

[1] Department of Astronomy, Peking University, Beijing 100871, China; *tianzhijia@pku.edu.cn; x.liu@pku.edu.cn*
[2] Department of Astronomy, Beijing Normal University, Beijing 100875, China
[3] National Astronomical Observatories, Chinese Academy of Sciences, Beijing 100101, China
[4] Department of Astronomy, Yunnan University, Kunming 650091, China

Received 2017 December 27; accepted 2018 February 7

Abstract Stellar systems composed of single, double, triple or higher-order systems are rightfully regarded as the fundamental building blocks of the Milky Way. Binary stars play an important role in formation and evolution of the Galaxy. Through comparing the radial velocity variations from multi-epoch observations, we analyze the binary fraction of dwarf stars observed with LAMOST. Effects of different model assumptions, such as orbital period distributions on the estimate of binary fractions, are investigated. The results based on log-normal distribution of orbital periods reproduce the previous complete analyses better than the power-law distribution. We find that the binary fraction increases with $T_{\rm eff}$ and decreases with [Fe/H]. We first investigate the relation between α-elements and binary fraction in such a large sample as provided by LAMOST. The old stars with high [α/Fe] dominate with a higher binary fraction than young stars with low [α/Fe]. At the same mass, earlier forming stars possess a higher binary fraction than newly forming ones, which may be related with evolution of the Galaxy.

Key words: binaries: general — binaries: spectroscopic — Galaxy: stellar content — stars: statistics — surveys

1 INTRODUCTION

Binary stars are common in the Galaxy (e.g., Duquennoy & Mayor 1991). They deserve to be considered when studying stellar kinematics, star formation rates (SFRs), initial mass functions and the occurrence of special stars, as aspects of the study of stellar populations. Given the light curves or radial velocity (RV) variations with time, binary stars provide an independent method to obtain stellar masses and radii using Kepler's third law, which offers exciting opportunities to develop highly constrained stellar models (e.g., Gorynya & Tokovinin 2014; Gaulme et al. 2016; Prša et al. 2016). Material and energy exchanges between the members of a binary system create the ideal breeding ground for the formation of some special stars, such as type Ia supernovae. Binary interactions make the appearance of the population substantially bluer, which affect the derived age and metallicity of the population (Zhang et al. 2007). Moreover, physical processes that are unique to close-in binary systems, such as mass exchange, are far from well understood.

It is important to identify binary stars or estimate binary fractions as a precondition to study properties of these stars. Several methods have been developed to detect binary stars, such as by means of RV, astrometric acceleration, direct imaging and common proper motion. Based on a complete sample of dwarf and subdwarf stars from the *Hipparcos* catalog (ESA 1997), Raghavan et al. (2010) analyze the multiplicity of solar-type stars out to 25 pc. They find that massive stars are more likely to have

⋆ LAMOST Fellow.

companions than less massive ones. Meanwhile, statistical analyses of quantities such as binary period distribution and mass-ratio distribution for binary systems are presented by Raghavan et al. (2010). Through the light curves obtained with *Kepler* (Borucki et al. 2010; Koch et al. 2010), a database[1] of 2876 eclipsing binaries (updated on 2017 April 27) has been constructed, including five groups: detached, semi-detached, over-contact, ellipsoidal binaries and uncertain (Matijevič et al. 2012). The probability of a star having a companion could be determined through comparing observed RVs with a single-star model and a binary-star model using the Markov chain Monte Carlo (MCMC) method (Hettinger et al. 2015), and metal-rich disk stars are found to be 30% more likely to have companions with periods shorter than 12 d than metal-poor halo stars. However, this method probably underestimates the fraction of binary stars. Rather than estimating the probability of a star having a companion, the total binary star fraction could be statistically measured by the dispersion of RVs from multi-epoch observations (Maoz et al. 2012; Gao et al. 2014, 2017). Single stars and binary stars have different distributions on a color-color diagram, thus the binary fraction of main sequence (MS) stars can also be estimated statistically through a stellar locus outlier (SLOT) method (Yuan et al. 2015b). Previous works by Gao et al. (2014, 2017) and Yuan et al. (2015b) show that metal-poor stars are more likely to possess companions than metal-rich ones. An analysis by Badenes et al. (2017) based on APOGEE data (Majewski et al. 2017) suggests that metal-poor stars have a multiplicity fraction a factor 2-3 higher than metal-rich stars, which is in qualitative agreement with the works of Gao et al. (2014, 2017) using low-resolution spectra of MS stars.

The multiplicity of F and G-type dwarf stars within 67 pc of the Sun with a completeness greater than 90% is presented by Tokovinin (2014a), and 80% of companions to the main targets in the sample are detected, which shows that the multiplicity fraction of the sample is about 46%. Shan et al. (2017) estimates the mean binary fraction of extremely young stars from young moving groups (YMGs) to be about 35^{+5}_{-4}%, which is lower than that of F and G-type field stars. Meanwhile, a combined analysis of multiplicity fraction as a function of mass and age over the ranges of 0.2 to 1.2 $M_{\odot}$ and 10 to 200 Myr respectively appears to be linearly flat in both parameters and across YMGs, which suggests constant multiplicity fractions from YMGs despite their differences in age and possibly birth environments (Shan et al. 2017). The binary fraction of white dwarf systems ($\sim 25\%$) within 20 pc is much lower compared to solar-type stars ($\sim 50\%$), which is explained by mergers in binary systems (Toonen et al. 2017). Research on the local white dwarf population within 25 pc suggests mechanisms that result in the loss of companions during binary system evolution (Holberg et al. 2016). The observed binary fraction is the combination of birth and dissipation rates of binary systems. In order to understand the observed binary fraction well, we had better estimate binary fractions of stars with different ages and evolutionary stages.

With the increase in quantity of data, more researches about binary stars can be carried out. In Section 2, we describe the method and assumptions adopted in this work. The data are presented in Section 3. The results are shown in Section 4, followed by discussions and conclusions in Section 5.

2 METHOD OF MEASURING BINARY STAR FRACTION

Binary systems can be detected through the dispersion of RVs (ΔRV) obtained with multi-epoch observations of the same stars. Through analyzing the distribution of the maximum RV difference ($\Delta\mathrm{RV}_{\mathrm{max}}$) between any two epochs for the same object, Maoz et al. (2012) statistically characterized binary fraction of a detached binary sample observed with the Sloan Digital Sky Survey (SDSS, York et al. 2000). The core of the $\Delta\mathrm{RV}_{\mathrm{max}}$ distribution is dominated by measurement errors, and the tail of the distribution is considered as a contribution from the binary population.

Although low-resolution spectra could not provide RV with high-enough precision to identify binarity for every star, we could statistically estimate binary fraction of a sample through a database of RV values from low-resolution spectra. Since the measurement of a quantity equals the true value plus the observational error, ΔRV for single stars is determined by the measurement uncertainty, while that for binary stars is determined by the phase of a binary system and the uncertainty in RVs of its members. Thus, the distributions of ΔRV would be described as (Gao et al. 2014)

$$\begin{aligned} p(\Delta\mathrm{RV}) =& f_{\mathrm{B}}\, p_{\mathrm{B}}(\Delta\mathrm{RV}|\sigma_{\mathrm{RV}}, \Delta t, M_{\mathrm{B}}) \\ &+ (1 - f_{\mathrm{B}})\, p_{\mathrm{S}}(\Delta\mathrm{RV}|\sigma_{\mathrm{RV}})\,, \end{aligned} \tag{1}$$

[1] Kepler Eclipsing Binary Catalog: *http://keplerebs.villanova.edu*

where $f_{\rm B}$ and $\sigma_{\rm RV}$ denote binary fraction and RV uncertainty, respectively, and Δt represents the time interval between two observations. $p_{\rm B}(\Delta{\rm RV}|\sigma_{\rm RV}, \Delta t, M_{\rm B})$ and $p_{\rm S}(\Delta{\rm RV}|\sigma_{\rm RV})$ represent probabilities of obtaining ΔRV under the assumptions of binary stars and single stars, respectively. Note that here we ignore the fraction of multiples (number of objects in the system $\geq$3), which is much lower than that of single or binary stars (Raghavan et al. 2010; Tokovinin 2014b).

For the binary systems $M_{\rm B}$, we suppose that: (1) the observed RVs are contributed from the primary stars of the binary systems; (2) their orbital orientations are considered as isotropic in three-dimensional (3D) space and initial phases follow uniform distributions. Meanwhile, the method adopted in this work is sensitive to orbital period distribution and mass ratio distribution of binary systems. In order to test effects of these distributions of binary stars on the determinations of $f_{\rm B}$ and $\sigma_{\rm RV}$, in this paper, we consider eight possible permutations of two models for the mass distribution of primary stars (Salpeter IMF and the mass distribution derived from isochrones), two models for the mass ratio distribution (a power-law distribution $f(q) \propto q^{\gamma}$ and a uniform distribution) and two models for the orbital period distribution ($\log P \sim N(5.03, 2.28^2)$ and $f(P) \propto P^{\alpha}$). An overview of these models is given in Table 1 and their details are explained below.

Two different mass distributions of primary stars are adopted in this work, one following the Salpeter IMF (Salpeter 1955), in which the masses of stars obey a power-law distribution, the other following the measured mass distribution of observed stars. Their masses and other fundamental parameters are determined by comparing the atmospheric parameters with the Yonsei-Yale (YY) isochrones (Demarque et al. 2004, and references therein). The details of estimating fundamental parameters are described in Section 4.3. As presented in Figure 1, the mass distribution of the whole sample shows a peak around 1 $M_{\odot}$ since the sample is not complete. For the mass ratio distributions, a power-law model $f(q) \propto q^{\gamma}$ (e.g. Raghavan et al. 2010, where $\gamma = 0.3 \pm 0.1$ for F, G and K-type MS stars) and a uniform distribution are adopted. For the orbital period distributions, a log-normal Gaussian profile (with a mean value of $\log P$ = 5.03 and a dispersion value of $\sigma_{\log P}$ = 2.28, where P is in units of days, see Raghavan et al. 2010) and a power-law distribution function $f(P) \propto P^{-1}$ (Öpik 1924; Abt 1983) are adopted for comparisons. Note that the distributions of periods and mass ratios in Raghavan et al. (2010) are derived from a highly complete sample of solar-type stars within 25 pc.

The time separations of multi-epoch observations in this work (with a typical value less than 5 yr) are much shorter than the mean periods of binary stars (with a typical period of about 300 yr, see Raghavan et al. 2010). The method adopted in this work is more sensitive to estimate the binary fraction of stars with short periods than long periods, but short-period binaries probably dominate circular or sub-orbicular orbits under the action of gravity. Thus, we ignore the distribution of eccentricities and assume circular orbits for binary systems in our study.

The distribution of Δt used in the calculation is that of stars considered in each bin. Given the distribution of Δt, the distribution of ΔRV would be a function of $f_{\rm B}$ and $\sigma_{\rm RV}$. Through the distribution $p(\Delta{\rm RV})$, we could estimate the binary fraction $f_{\rm B}$ and the mean error of RVs $\sigma_{\rm RV}$, with a maximum likelihood estimation method. The uncertainties in RVs are functions of signal to noise ratio (SNR), $T_{\rm eff}$, $\log g$ and [Fe/H] (Xiang et al. 2015). For single stars with similar SNR, $T_{\rm eff}$, $\log g$ and [Fe/H], the distribution of ΔRV follows a Gaussian distribution. However, the distribution of ΔRV for binary stars does not follow a Gaussian distribution, because the RV varies with time or phase of a binary system. The wings of the distribution overlapping the Gaussian profile are engendered from the contribution of binary stars. Thus, we could estimate the fraction of binary stars through the distribution of ΔRV. However, the combinations of ΔRV with different dispersions could also be used to deduce wings overlapping a Gaussian profile. There is some degeneracy between $f_{\rm B}$ and $\sigma_{\rm RV}$. To minimize the effects of $\sigma_{\rm RV}$ dispersions on the estimation of $f_{\rm B}$, it is necessary to construct subsamples with similar $\sigma_{\rm RV}$. Therefore, only data with SNR greater than 50 are used in the analyses. Meanwhile, we estimate binary star fractions in multi-dimensional bins of $T_{\rm eff}$, [α/Fe] and [Fe/H]. Note that the primary mass distributions in each bin differ because of the restrictions of $T_{\rm eff}$, [α/Fe] and [Fe/H]. To ensure validity of the estimation, we only consider bins with numbers of stars over 1500.

3 DATA

With progress related to the Large Sky Area Multi-Object Fiber Spectroscopic Telescope (LAMOST) spectroscopic survey (Cui et al. 2012; Zhao et al. 2012; Deng et al. 2012; Liu et al. 2014; Yuan et al. 2015a), more and

Table 1 The Assumptions of Period Distribution, Primary Mass and Mass Ratio

Model No.	Orbital period distribution	Primary mass distribution	Mass ratio distribution
1	$\log P \sim N(5.03, 2.28^2)$ [a]	$\xi(M) = \xi_0 M^{-2.35}$ [c]	$f(q) \propto q^{0.3\pm0.1}$ [a]
2	$\log P \sim N(5.03, 2.28^2)$ [a]	$\xi(M) = \xi_0 M^{-2.35}$ [c]	uniform distribution
3	$\log P \sim N(5.03, 2.28^2)$ [a]	masses from the sample [d]	$f(q) \propto q^{0.3\pm0.1}$ [a]
4	$\log P \sim N(5.03, 2.28^2)$ [a]	masses from the sample [d]	uniform distribution
5	$f(P) \propto P^{-1}$ [b]	$\xi(M) = \xi_0 M^{-2.35}$ [c]	$f(q) \propto q^{0.3\pm0.1}$ [a]
6	$f(P) \propto P^{-1}$ [b]	$\xi(M) = \xi_0 M^{-2.35}$ [c]	uniform distribution
7	$f(P) \propto P^{-1}$ [b]	masses of the sample [d]	$f(q) \propto q^{0.3\pm0.1}$ [a]
8	$f(P) \propto P^{-1}$ [b]	masses of the sample [d]	uniform distribution

Notes: [a] Raghavan et al. (2010); [b] Öpik (1924); Abt (1983); [c] Salpeter (1955); [d] Masses of the sample derived from theoretical isochrones.

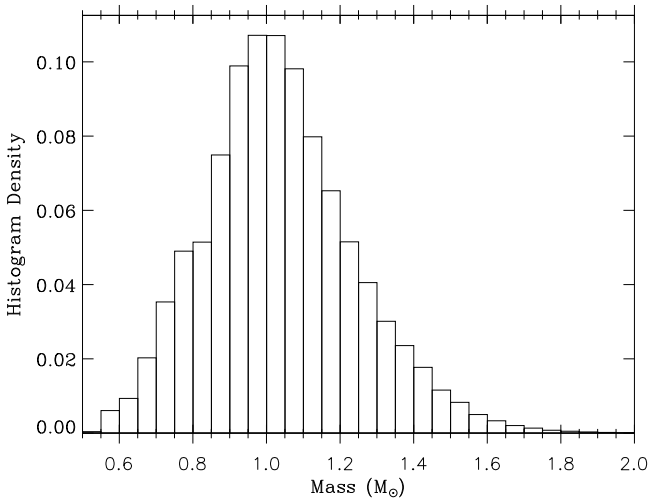

Fig. 1 Mass distribution of stars adopted in this work.

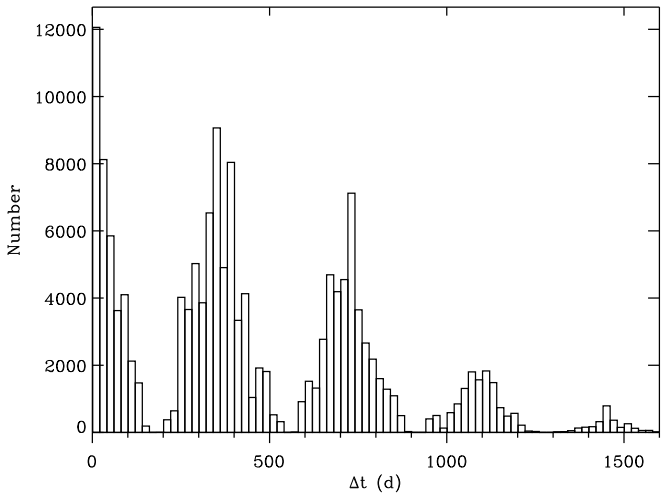

Fig. 2 Time interval distribution of 0.15 million stars used in this work.

more stars have been observed more than once, providing a great opportunity for studies of field binaries. About 4 million unique objects marked with 'star' have been targeted by November, 2016, and over 0.93 million unique stars with SNR greater than 10 have been observed with two or more epochs. The data are contained in LAMOST Data Release 4 (DR4). To obtain atmospheric parameters and RVs of stars, stellar parameter pipelines such as the LASP (Wu et al. 2011) and the LSP3 (Xiang et al. 2015, 2017) have been developed and applied to LAMOST spectra. We adopt the stellar parameters yielded by LSP3 for F, G and K-type stars observed with LAMOST (by November, 2016).

We focus on the binary fractions of F, G and K-type MS stars. In order to remove giant stars from the sample, a cut of $\log g > 3.75$ is adopted. The $T_{\rm eff}$ of the selected sample is limited in the range of 4000–7000 K. Observations taken during the same night probably share similar conditions (e.g. seeing, skylight, flat), and the measured velocities share similar systematic errors. Therefore, the data with time intervals less than one day are excluded in this work to make sure that multi-epoch observations for each star were carried out in different nights. For most binary stars, the periods are about dozens to hundreds of years. Thus, the method is more sensitive to multi-epoch observations with long time intervals than short ones. In principle, RVs with high SNR and large time separation of multi-epoch observations are required to carry out the work. For stars observed more than twice, we obtain a vector of $\mathrm{RV} = \{\mathrm{RV}_1, \mathrm{RV}_2, ..., \mathrm{RV}_n\}$ which is a response for a vector of time $t = \{t_1, t_2, ..., t_n\}$. We select the two RVs which dominate the maximum value of $\mathrm{SNR}_j * \mathrm{SNR}_k * (t_j - t_k)$. We obtain about 0.15 million stars observed at least two times and with time interval larger than one day and SNR greater than 50. The time interval distribution of multi-epoch observations for the sample is presented in Figure 2. The maximum of time interval is about 1600 d.

4 BINARY FRACTIONS IN PARAMETER SPACES

The sample is divided into subsamples with 3D bins of $T_{\rm eff}$, [Fe/H] and [α/Fe]. The binning widths of these quantities are 500 K, 0.2 dex and 0.2 dex with overlaps of 250 K, 0.1 dex and 0.1 dex, respectively. The binary fractions are estimated for each subsample and under different model assumptions, as listed in Table 1. For example, Figure 3 shows the contours of the likelihood of $\sigma_{\rm RV}$ and $f_{\rm B}$ for stars with $T_{\rm eff}$ in the range of 5000–5500 K, [Fe/H] in the range of $-0.10 \sim 0.10$ dex and [α/Fe] in the range of $-0.10 \sim 0.10$ dex. The estimation is performed under the assumptions of Model 1. The two-dimensional (2D) joint probability is converted into probabilities of $\sigma_{\rm RV}$ and $f_{\rm B}$, namely $p(\sigma_{\rm RV})$ and $p(f_{\rm B})$, respectively. The values of $\sigma_{\rm RV}$ and $f_{\rm B}$ and their 1-sigma errors are estimated accordingly. Our result, $f_{\rm B} = 55^{+4}_{-2}\%$, is consistent with previous work (e.g. Raghavan et al. 2010). A comparison between observed and simulated ΔRV distributions is plotted on Figure 4. As shown on the bottom panel of the figure, the residual is below 1%.

4.1 The Effects of Different Assumptions on the Estimation of Binary Fractions

In order to compare the results under different assumptions, we plot the binary fractions versus $T_{\rm eff}$ and [Fe/H] for stars of $-0.1 < [\alpha/\mathrm{Fe}] < 0.1$ based on Models 1–4 in Figure 5 and Models 5–8 in Figure 6. All models in Figure 5 are based on the log-normal distribution of orbital periods (Raghavan et al. 2010), but assuming different mass distributions of the primary stars and mass ratio distributions.

For Models 1–4, the discrepancies in $f_{\rm B}$ are below 10 percent. For Models 5–8, the estimated $f_{\rm B}$ values based on the power-law distribution of orbital period are about half of those based on the log-normal Gaussian distribution. This is because binary systems described by Models 5–8 have a larger fraction of short-period binaries than Models 1–4. The statistical analysis of the complete sample within 25 pc suggests that the binary fraction of solar-type stars is about 50% (Raghavan et al. 2010), which supports the result based on the log-normal Gaussian distribution of orbital periods. In the following analyses, we only consider the results based on Models 1–4.

Given the orbital periods following the log-normal distribution, $f_{\rm B}$ values estimated based on different primary mass distributions and mass ratio distributions differ slightly. Models with the same orbital period distribution and the same primary mass distribution as Models 1 and 2 (or Models 3 and 4) show that $f_{\rm B}$ estimated under the mass ratio distribution of a power-law index is higher than that based on a uniform distribution. This is because given the period and mass ratio distributions, binary systems with high primary mass will obtain a large separation and a high velocity.

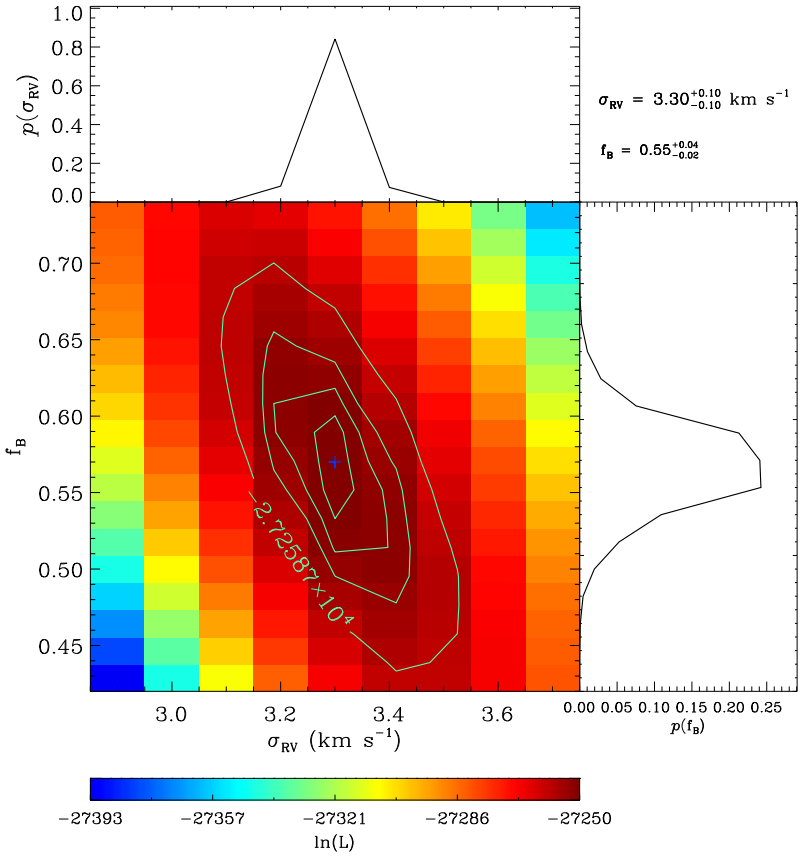

Fig. 3 Likelihood of $\sigma_{\rm RV}$ and $f_{\rm B}$ for stars with $T_{\rm eff}$ in the range of $5000 - 5500$ K, [Fe/H] in the range of $-0.10 \sim 0.10$ dex and [α/Fe] in the range of $-0.10 \sim 0.10$ dex. The *top* and *right* panels present the probabilities of $\sigma_{\rm RV}$ and $f_{\rm B}$, respectively. The values of $\sigma_{\rm RV}$ and $f_{\rm B}$ with 1-sigma error are shown on the *upper-right*.

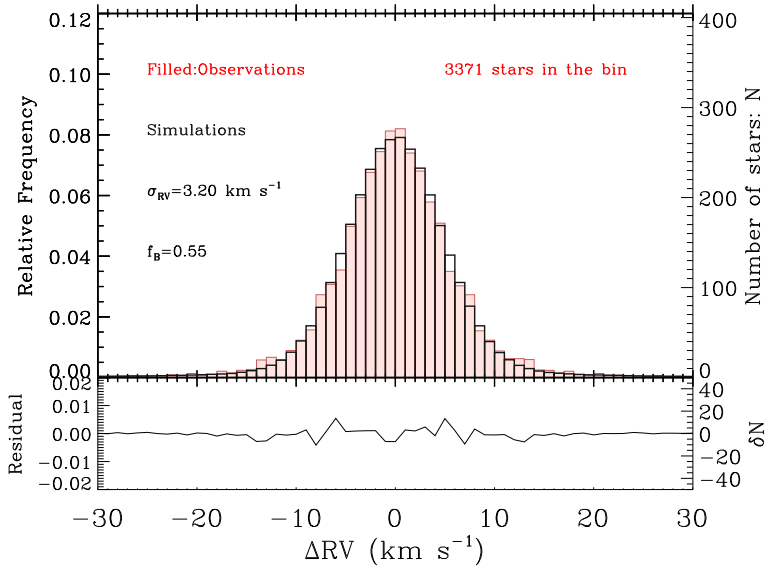

Fig. 4 The *top panel* shows the observed (*red-filled*) and fitted (*black-unfilled*) ΔRV distribution for solar-type stars. The residuals are plotted in the *bottom panel*.

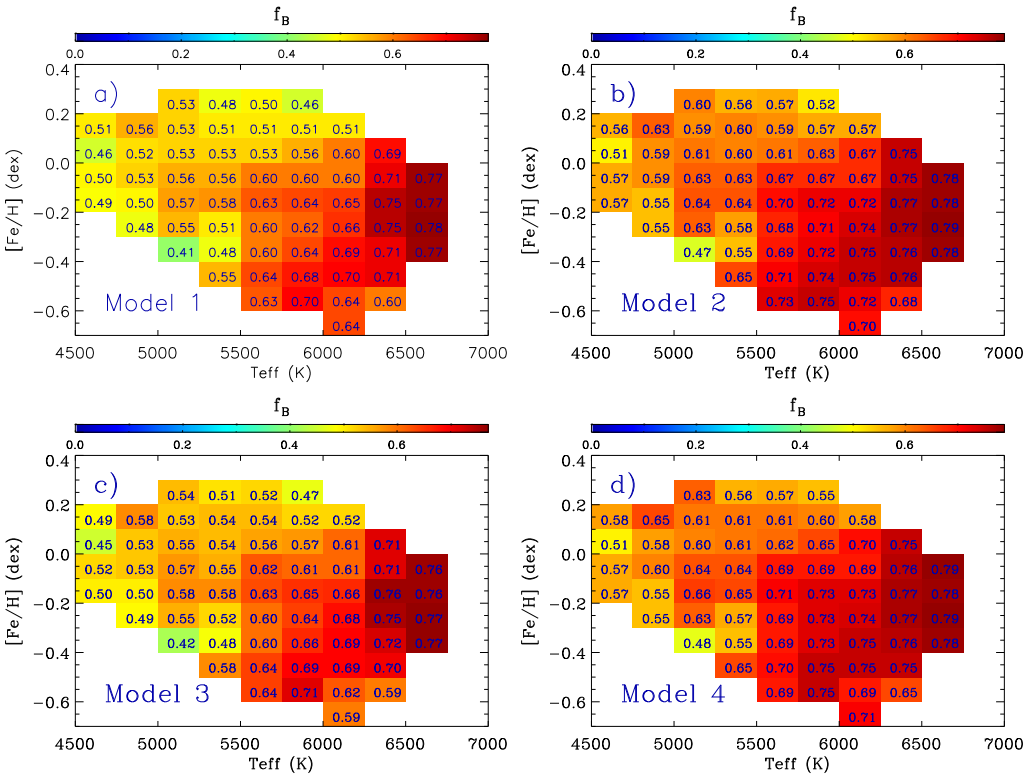

Fig. 5 Binary fractions of stars on the $T_{\rm eff}$-[Fe/H] panel under different model assumptions. Colors denote the values of binary fractions in different bins. The errors in $f_{\rm B}$ are below 10%.

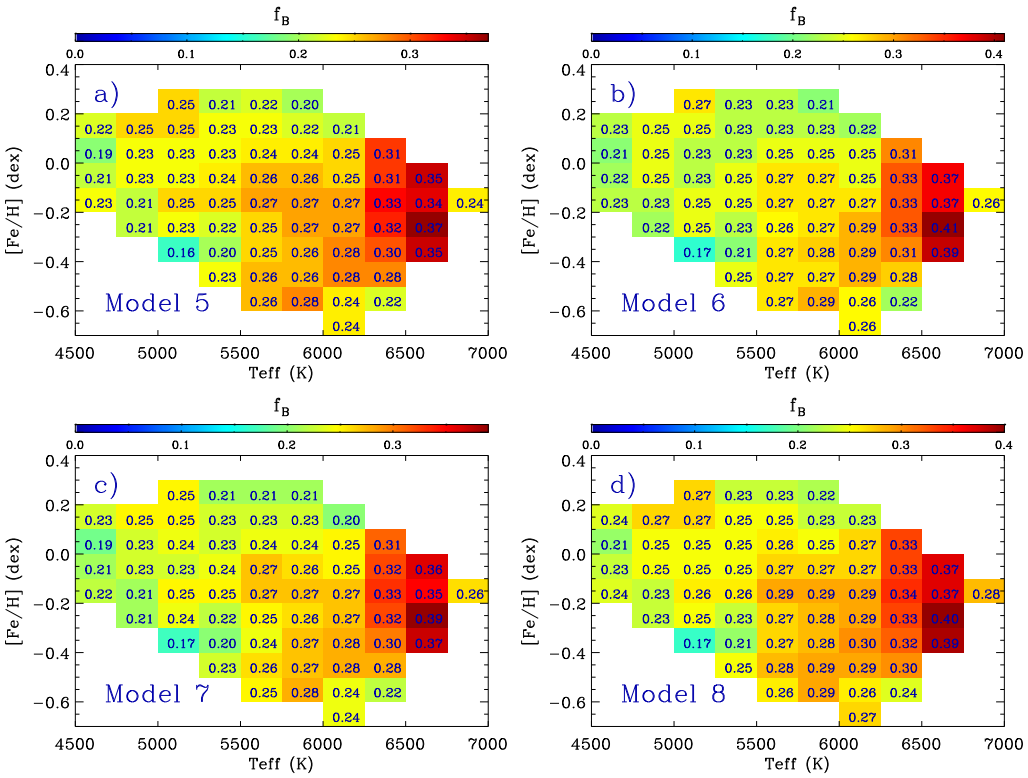

Fig. 6 Same as Fig. 5, but for Models 5–8.

Comparing Models 1 and 3 (or Models 2 and 4), we find that the $f_{\rm B}$ estimated under the primary mass distribution of the Salpeter (1955) IMF is slightly lower than that based on the mass distribution of the sample. The order of mean $f_{\rm B}$ from large to small is Models 4, 2, 3 and 1. Even the difference in $f_{\rm B}$ between Models 1 and 4 is lower than 10 percent.

4.2 Binary Fractions on the $T_{\rm eff}$-[Fe/H] Panel

As shown in all panels of Figure 5, for a given value of [Fe/H], the binary fraction increases as $T_{\rm eff}$ increases for MS stars. For a given value of $T_{\rm eff}$, the binary fraction decreases as [Fe/H] increases. There is a positive gradient of binary fractions from the top left to bottom right in the $T_{\rm eff}$-[Fe/H] panel. The results agree well with those of Gao et al. (2017).

As described in Xiang et al. (2015), the $\sigma_{\rm RV}$ variation is a function of SNR, $T_{\rm eff}$ and [Fe/H]. In Figure 7, of $\sigma_{\rm RV}$ in the $T_{\rm eff}$-[Fe/H] panel corresponding to $f_{\rm B}$ in Figure 5. We find a positive correlation coefficient between $\sigma_{\rm RV}$ and $f_{\rm B}$ of about 0.70. There is a strong negative correlation between $\sigma_{\rm RV}$ and $f_{\rm B}$, as shown in Figure 3, suggesting the trend of $f_{\rm B}$ versus $T_{\rm eff}$ and [Fe/H] is not caused by the trend of $\sigma_{\rm RV}$ versus stellar parameters.

4.3 Binary Fractions Versus Star Formation Time

According to the theory of stellar evolution, high-mass stars evolve faster than low-mass ones during the MS phase. The typical age of high-mass MS stars is younger than low-mass ones. The phenomenon that binary fractions of high-$T_{\rm eff}$ stars is higher than those of low-$T_{\rm eff}$ MS stars is probably related to the variation of $f_{\rm B}$ versus masses or formation times of stars. Given a star's current age, we can trace the time of its formation. The older a star is, the earlier it formed. To study the binary fractions in stellar parameter spaces, it is necessary to obtain the fundamental parameters such as mass and formation time of stars. For each MS star, we start by using [Fe/H], [α/Fe], $T_{\rm eff}$ and $\log g$ to get an estimate of the mass (M) and formation time (t) of the star using the Yale-Birmingham grid-based modeling pipeline (Basu et al. 2010), which estimates stellar properties by comparing observed quantities to the outputs of stellar evolutionary models. The grid-based stellar models adopted in this work are from YY isochrones (Demarque et al. 2004, and references therein), which consider the effects of [α/Fe].

Figure 8 presents the binary fraction variations with metallicities and α-element abundances for stars with $T_{\rm eff}$ in the range of 5500–6000 K. The $\sigma_{\rm RV}$ variations corresponding to Models 1–4 in Figure 8 are presented in Figure 9. For α-poor stars, it shows the trend that binary fractions increase with the decrease of [Fe/H], which agrees with Figure 5. For α-rich stars, the binary fractions show obvious variations with [Fe/H]. There is a macroscopical trend that the α-rich stars possess higher $f_{\rm B}$ than α-poor stars. Since elemental abundances are indicators of star formation time, the variations of binary fractions versus elemental abundances reflect the variation of binary fractions with time, which may be related to evolution of the Galaxy.

In order to test the changes of binary fraction with star formation time directly, we estimate the binary fractions in 2D bins of mass and star formation time. We select samples of low-mass stars formed 1–8 Gyr ago with [Fe/H] in the range of $-0.1 \sim 0.1$ dex. The selected stars between 0.8 and 1.2 $M_{\odot}$ are divided into two bins of equal width in mass. The relative errors of mass and formation time are about below 10% and 50% for this sample, respectively.

Figure 10 presents the binary fraction as a function of star formation time. It shows that the earlier forming stars possess a higher binary fraction than newly forming ones. Given the mass difference of 0.2 $M_{\odot}$, the binary fraction of high-mass stars is higher than that of low-mass stars. Note that the SFRs based on integrated-light analyses and stellar color-magnitude diagrams show good agreement that SFR is a function of time (Ruiz-Lara et al. 2015). More researches should be carried out to study the relation between the initial binary fraction and SFR.

5 CONCLUSIONS AND DISCUSSIONS

In this paper, we estimate the binary fractions $f_{\rm B}$ of 0.15 million dwarf stars observed with LAMOST. The estimated $f_{\rm B}$ of the sample stars is sensitive to the adopted assumptions of mass function, mass ratio distribution and period distribution. The estimated $f_{\rm B}$ of about 50% for solar-type stars based on the log-normal distribution of orbital periods is coincident with previous statistical analysis of a complete sample within 25 pc (e.g. Raghavan et al. 2010). Not only in a small sample, but also in such a large sample of survey data do the orbital periods of binary stars prefer a log-normal distribution to other ones.

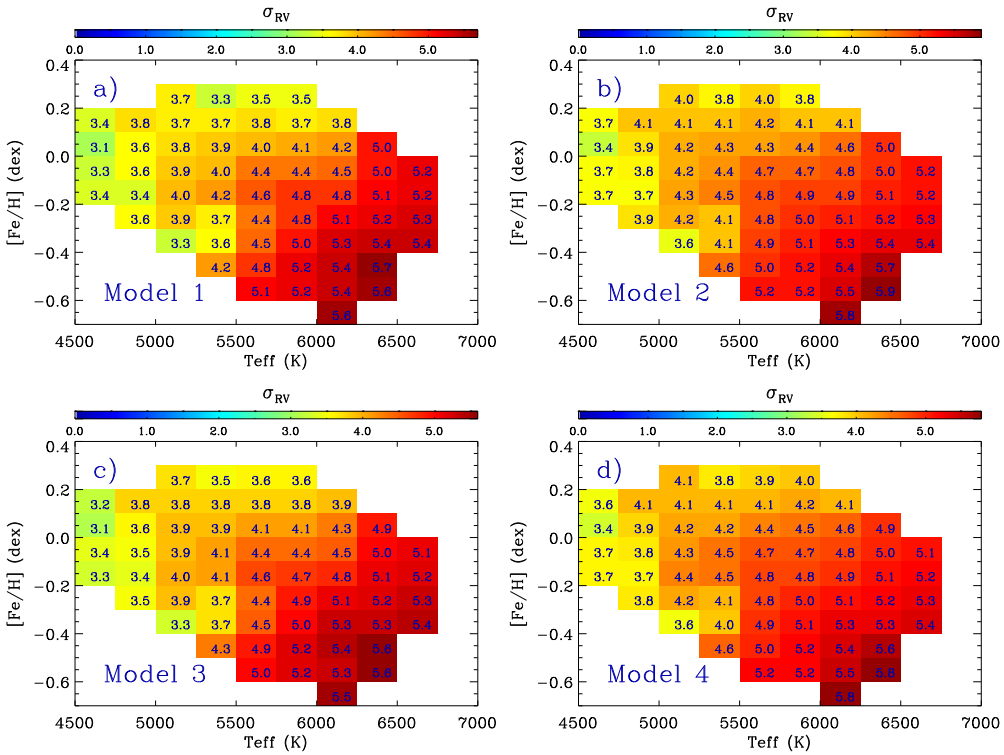

Fig. 7 Uncertainties in RV versus $T_{\rm eff}$-[Fe/H]. Panels *a* - *d* present the $\sigma_{\rm RV}$ estimated based on Models 1–4 in Fig. 5, respectively. The colors denote the values of $\sigma_{\rm RV}$ in different bins.

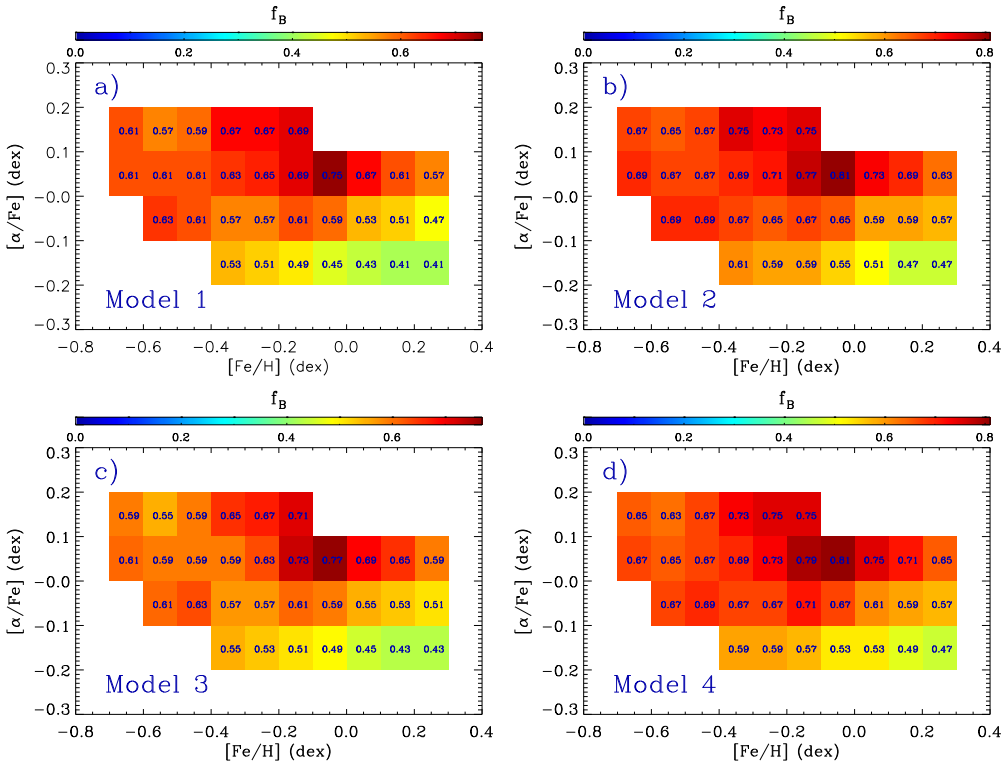

Fig. 8 Binary fractions of stars with $T_{\rm eff}$ in the range of 5500–6000 K in the [Fe/H]-[α/Fe] panel. Colors denote the values of binary fractions in different bins.

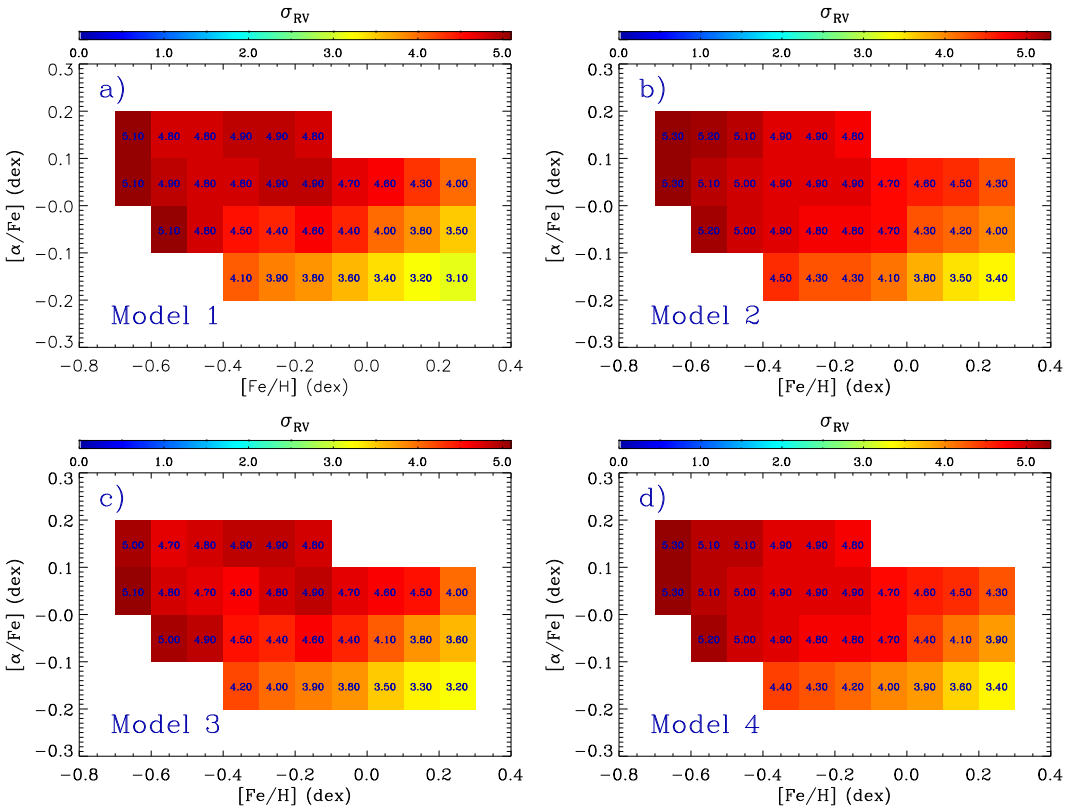

Fig. 9 The uncertainty in RV versus [Fe/H]-[α/Fe]. Panels (a)–(d) present $\sigma_{\rm RV}$ estimated based on Models 1–4 in Fig 8, respectively. Colors denote the values of $\sigma_{\rm RV}$ in different bins.

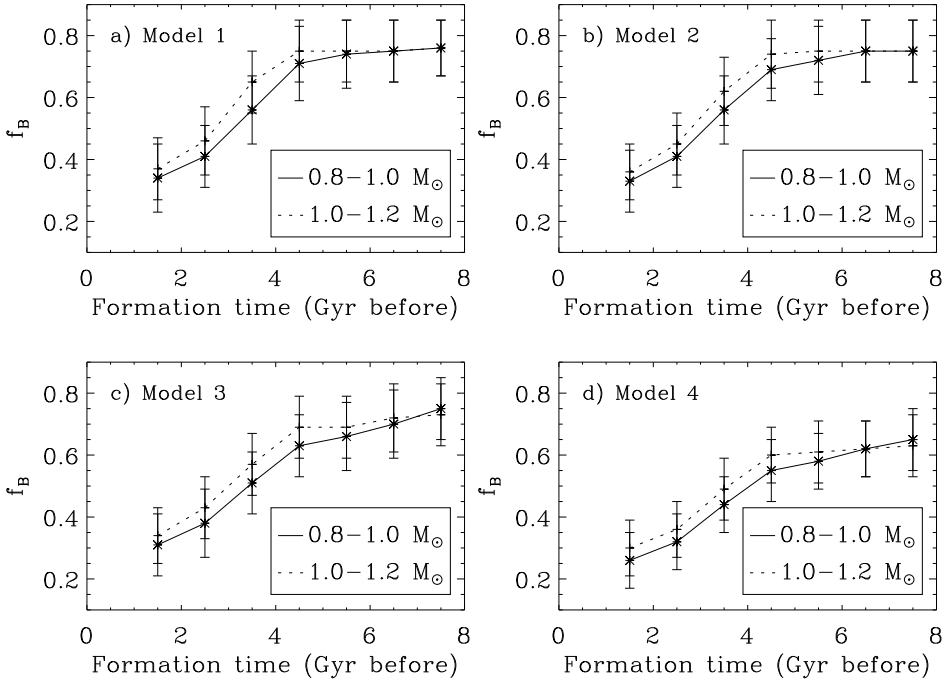

Fig. 10 Binary fraction as a function of star formation time. The range of metallicity is $-0.1 \sim 0.1$ dex.

The binary fractions increase with the increase of $T_{\rm eff}$ and the decrease of [Fe/H]. We first investigate the relation between α-elements and binary fraction in such a large sample as provided by LAMOST. The old stars with high [α/Fe] have a higher binary fraction than young stars with low [α/Fe]. The variations of binary fraction with star formation time may be related with the evolution of the Galaxy.

This work is based on the assumption that RVs of binary stars are derived from the spectra of primary stars. Binaries with similar components are difficult to detect, since their spectra are blended. However, this bias does not change the trend of binary fractions in space bins. The effects of spectral blend on estimating binary fractions will be discussed in our future work.

With the progresses of sky-surveys such as SDSS (York et al. 2000) and LAMOST (Cui et al. 2012; Zhao et al. 2012), RVs of more and more stars could be derived from spectra. RVs from spectral surveys together with parallaxes from Gaia (Gaia Collaboration et al. 2016) enable researches about binary stars that are not limited to a small sample of data. Large sample analysis of binary stars will improve our knowledge about binary star formation and dissipation all over the Milky Way. In future work, we plan to identify binary stars through their RV and proper motion variations. From the LAMOST and Gaia data on millions of stars, a huge gallery of identified binary stars can be established. An enormous number of binary stars will be used to trace the evolution of Galactic stellar populations.

Acknowledgements This work has made use of data products from the Guo Shou Jing Telescope (the Large Sky Area Multi-Object Fiber Spectroscopic Telescope, LAMOST). LAMOST is a National Major Scientific Project built by the Chinese Academy of Sciences. Funding for the project has been provided by the National Development and Reform Commission. LAMOST is operated and managed by National Astronomical Observatories, Chinese Academy of Sciences.

This work is partially supported by the National Key Basic Research Program of China (2014CB845700), China Postdoctoral Science Foundation (2016M600850), the National Natural Science Foundation of China (No. 11443006) and Joint Research Fund in Astronomy (Nos. U1531244 and U1631236). The LAMOST fellowship is supported by Special Funding for Advanced Users, budgeted and administrated by the Center for Astronomical Mega-Science, Chinese Academy of Sciences (CAMS).

References

Abt, H. A. 1983, ARA&A, 21, 343
Badenes, C., Mazzola, C., Thompson, T. A., et al. 2017, arXiv:1711.00660
Basu, S., Chaplin, W. J., & Elsworth, Y. 2010, ApJ, 710, 1596
Borucki, W. J., Koch, D., Basri, G., et al. 2010, Science, 327, 977
Cui, X.-Q., Zhao, Y.-H., Chu, Y.-Q., et al. 2012, RAA (Research in Astronomy and Astrophysics), 12, 1197
Demarque, P., Woo, J.-H., Kim, Y.-C., & Yi, S. K. 2004, ApJS, 155, 667
Deng, L.-C., Newberg, H. J., Liu, C., et al. 2012, RAA (Research in Astronomy and Astrophysics), 12, 735
Duquennoy, A., & Mayor, M. 1991, A&A, 248, 485
ESA, ed. 1997, ESA Special Publication, 1200, The HIPPARCOS and TYCHO Catalogues. Astrometric and Photometric Star Catalogues Derived from the ESA HIPPARCOS Space Astrometry Mission
Gaia Collaboration, Prusti, T., de Bruijne, J. H. J., et al. 2016, A&A, 595, A1
Gao, S., Liu, C., Zhang, X., et al. 2014, ApJ, 788, L37
Gao, S., Zhao, H., Yang, H., & Gao, R. 2017, MNRAS, 469, L68
Gaulme, P., McKeever, J., Jackiewicz, J., et al. 2016, ApJ, 832, 121
Gorynya, N. A., & Tokovinin, A. 2014, MNRAS, 441, 2316
Hettinger, T., Badenes, C., Strader, J., Bickerton, S. J., & Beers, T. C. 2015, ApJ, 806, L2
Holberg, J. B., Oswalt, T. D., Sion, E. M., & McCook, G. P. 2016, MNRAS, 462, 2295
Koch, D. G., Borucki, W. J., Basri, G., et al. 2010, ApJ, 713, L79
Liu, X.-W., Yuan, H.-B., Huo, Z.-Y., et al. 2014, in IAU Symposium, 298, Setting the Scene for Gaia and LAMOST, eds. S. Feltzing, G. Zhao, N. A. Walton, & P. Whitelock, 310
Majewski, S. R., Schiavon, R. P., Frinchaboy, P. M., et al. 2017, AJ, 154, 94
Maoz, D., Badenes, C., & Bickerton, S. J. 2012, ApJ, 751, 143
Matijevič, G., Prša, A., Orosz, J. A., et al. 2012, AJ, 143, 123
Öpik, E. 1924, Publications of the Tartu Astrofizica Observatory, 25, 1
Prša, A., Conroy, K. E., Horvat, M., et al. 2016, ApJS, 227, 29
Raghavan, D., McAlister, H. A., Henry, T. J., et al. 2010, ApJS, 190, 1
Ruiz-Lara, T., Pérez, I., Gallart, C., et al. 2015, A&A, 583, A60
Salpeter, E. E. 1955, ApJ, 121, 161

Shan, Y., Yee, J. C., Bowler, B. P., et al. 2017, ApJ, 846, 93
Tokovinin, A. 2014a, AJ, 147, 86
Tokovinin, A. 2014b, AJ, 147, 87
Toonen, S., Hollands, M., Gänsicke, B. T., & Boekholt, T. 2017, A&A, 602, A16
Wu, Y., Luo, A.-L., Li, H.-N., et al. 2011, RAA (Research in Astronomy and Astrophysics), 11, 924
Xiang, M. S., Liu, X. W., Yuan, H. B., et al. 2015, MNRAS, 448, 822
Xiang, M.-S., Liu, X.-W., Shi, J.-R., et al. 2017, MNRAS, 464, 3657
York, D. G., Adelman, J., Anderson, Jr., J. E., et al. 2000, AJ, 120, 1579
Yuan, H.-B., Liu, X.-W., Huo, Z.-Y., et al. 2015a, MNRAS, 448, 855
Yuan, H., Liu, X., Xiang, M., et al. 2015b, ApJ, 799, 135
Zhang, F., Han, Z., & Li, L. 2007, in IAU Symposium, 241, Stellar Populations as Building Blocks of Galaxies, ed. A. Vazdekis & R. Peletier, 205
Zhao, G., Zhao, Y.-H., Chu, Y.-Q., Jing, Y.-P., & Deng, L.-C. 2012, RAA (Research in Astronomy and Astrophysics), 12, 723